Journal of Applied Toxicology

WILEY

Journal of AppliedToxicology

RESEARCH ARTICLE

Ergothioneine Ameliorates Liver Fibrosis by Inhibiting Glycerophospholipids Metabolism and TGF-β/Smads Signaling Pathway: Based on Metabonomics and Network Pharmacology

Yaping Mao[1] | Zhenghui Xie[1] | Xiangxia Zhang[2,3] | Yu Fu[1] | Xiaotong Yu[2] | Lili Deng[1] | Xiu Zhang[2] | Bo Hou[3] | Xiao Wang[4] | Mingyue Ma[1] | Fu Ren[2,5,6]

[1]Department of Toxicology, School of Public Health, Shenyang Medical College, Shenyang, China | [2]Department of Anatomy, School of Basic Medicine, Shenyang Medical College, Shenyang, China | [3]Department of Morphology, School of Nursing and Health, Qingdao Huanghai University, Qingdao, China | [4]Department of Gastroenterology, Central Hospital Affiliated to Shenyang Medical College, Shenyang, China | [5]Key Laboratory of Human Ethnic Specificity and Phenomics of Critical Illness in Liaoning Province, Shenyang Medical College, Shenyang, China | [6]Key Laboratory of Phenomics in Shenyang, Shenyang Medical College, Shenyang, China

Correspondence: Mingyue Ma (mymacmu@163.com) | Fu Ren (rf@symc.edu.cn)

Received: 22 September 2024 | **Revised:** 23 October 2024 | **Accepted:** 6 November 2024

Funding: This work was supported by the Central Government Guides Local Science and Technology Development Fund (No. 2023JH6/100100021), Special Professor Project in Liaoning Province (No. LNTP20183501), Society Service Station of Shenyang Medical College, and Science and Technology Innovation Fund for Postgraduates of Shenyang Medical College (No. Y20220517).

Keywords: ergothioneine | inflammation | liver fibrosis | metabonomics | network pharmacology | TGF-β/Smads

ABSTRACT

Ergothioneine (EGT) is a diet-derived natural sulfur-containing amino acid that exhibits strong anti-oxidant and anti-inflammation activities. Oxidative stress and chronic inflammatory injury are predominant pro-fibrogenic factors. Therefore, EGT may have therapeutic potential against liver fibrosis; however, its underlying mechanism is incompletely understood. This study aimed at investigating the protective effects of EGT on liver fibrosis based on metabonomics and network pharmacology. A mouse model of liver fibrosis was established by intraperitoneal injection with 40% CCl_4 solution (2 mL/kg, twice a week) and intragastric administration with EGT (5, 10 mg/kg/d) for six weeks. Results showed that EGT improved liver function by reducing serum levels of ALT (alanine aminotransferase), AST (aspartate aminotransferase), and TBIL (total bilirubin), and alleviated liver fibrosis by reducing LN (laminin) and HyP (hydroxyproline) levels, decreasing expressions of α-SMA (α-smooth muscle actin), Col-I (collagen type I), and Col-III (collagen type III), and improving pathological changes. EGT also significantly inhibited CCl_4-induced hepatic inflammation and TGF-β/Smads signaling pathway. Metabolomics identified six key metabolic pathways, such as purine metabolism, glycerophospholipid metabolism, and sphingolipid metabolism, and eight key metabolites, such as xanthine, guanine, ATP, phosphatidylcholine, and sphingosine. Network pharmacology analysis showed that IL-17, cAMP and NF-κB signaling pathways were potential key mechanisms. Integrated analysis revealed that PLA2G2A might be a potential target of EGT against liver fibrosis. EGT may inhibit the glycerophospholipid metabolism through PLA2G2A to inhibit the TGF-β/Smads signaling pathway, thereby alleviating fibrosis. The present study indicates that EGT may be considered a valid therapeutic strategy to regress liver fibrosis, and provides novel insights into the pharmacological mechanism of EGT against liver fibrosis.

Yaping Mao, Zhenghui Xie, and Xiangxia Zhang: These authors have contributed equally to this work and share first authorship.

1 | Introduction

Worldwide, approximately 2 million people die from liver fibrosis every year, making it a major public health challenge (Asrani et al. 2019). The degree of fibrosis is related to the progression and prognosis of liver disease, and it is the major risk factor affecting the outcome of liver disease (Roehlen, Crouchet, and Baumert 2020). Hepatic fibrosis is an inflammatory response to chronic liver injury caused by viral hepatitis, alcohol consumption, autoimmune hepatitis, non-alcoholic steatohepatitis (NASH), or cholestatic liver disease (Aydın and Akçalı 2018). Chronic inflammatory injury in the liver can persistently induce the transdifferentiation of hepatic stellate cells (HSCs) to myofibroblasts, which secrete excessive fibrillar extracellular matrix (ECM) proteins, e.g., collagen type I (Col-I) and III (Col-III), that generate the fibrous scar (Kisseleva and Brenner 2021). Clinical and experimental data have shown that when the causative agents are removed, liver fibrosis is reversible, which is associated with the reduction of inflammatory factors, eradication of activated myofibroblasts, and resorption of fibrous scar tissue (Campana and Iredale 2017; Sun and Kisseleva 2015). The balance of pro-fibrogenic and anti-fibrogenic mechanisms is regulated by cytokine-induced signaling pathways, such as TGF-β (Cheng et al. 2019), NF-κB (de Gregorio et al. 2020), NLRP3 inflammasome pathway (Charan et al. 2022), and Wnt/β-catenin signaling (Nishikawa, Osawa, and Kimura 2018). As of yet, no direct antifibrotic therapy has been approved. A new drug target or candidate to prevent or treat liver fibrosis early is extremely important for chronic liver disease prognosis.

Antifibrotic therapies aim to inhibit the accumulation of fibrogenic cells and prevent the deposition of ECM proteins. Edible plant-derived natural compounds, including sulfur-containing compounds, have been demonstrated to exert antifibrotic effects without causing side effects, and can be used as complementary and alternative therapies for fibrosis treatment (Milito et al. 2019). L-Ergothioneine (EGT) is a thio-histidine betaine amino acid and was first identified from the ergot fungus *Claviceps purpurea* 1 (Tang et al. 2018). Biosynthesis of EGT has been only observed in some fungi and bacteria. Therefore, in humans, EGT is mainly obtained from diet, such as mushrooms (Tang et al. 2018). It can be taken up into cells by a specific transporter SLC22A4, and accumulates in several tissues such as liver, blood, kidneys, spleen, and lungs (Gründemann, Hartmann, and Flögel 2022; Tang et al. 2018). After oral administration, the concentration of EGT can be increased in plasma and whole blood, meanwhile, oxidative damage biomarkers are decreased (Cheah et al. 2017). Therefore, EGT is a powerful physiological antioxidant that scavengers free radicals, interacts with the body's natural antioxidant defense system, and chelates divalent metal cations (Fu and Shen 2022). There is evidence that EGT may maintain a high level at sites of tissue injury induced by inflammation and oxidative stress by increasing SLC22A4 levels (Halliwell, Cheah, and Tang 2018). A growing body of evidence suggests that EGT may be an important dietary intervention for inflammatory diseases, and is suggested as a food supplement (longevity vitamin) (Ames 2018; Tian, Thorne, and Moore 2023).

Notably, liver is the main tissue for accumulating EGT, however, there is limited information regarding EGT's potential to mitigate liver fibrosis. EGT has potent anti-oxidant activities and provides significant prevention against oxidative stress in tissues (Borodina et al. 2020). It was found that EGT appears to provide protection against peroxidation injury to the liver as well as reducing consumption of endogenous glutathione and tocopherols (Deiana et al. 2004). A guinea pig model of non-alcoholic fatty liver disease (NAFLD) accumulates EGT by upregulating its transporter, possibly as a stress response by damaged livers to further suppress oxidative stress (Cheah et al. 2016). In addition, EGT has also exhibited the ability to modulate inflammation. Dare, Channa, and Nadar (2021) reported that EGT could reduce liver injury, oxidative stress, and inflammation in diabetic rats. It is well recognized that the progression of liver fibrosis is primarily influenced by oxidative stress and chronic inflammatory injury (Banerjee et al. 2023). Therefore, EGT may be therapeutic for liver fibrosis through its anti-oxidant and anti-inflammatory effects, however, its underlying mechanism is incompletely understood.

Network pharmacology is a new discipline to identify potential molecular mechanisms of drugs in treating related diseases (Chen et al. 2023). In addition, metabonomics analysis reflects the species and quantities of endogenous metabolites (<1500 Da) caused by pathophysiological changes or external stimuli in organisms (Qin et al. 2023). Comprehensive analysis of these changes can reveal the metabolic activities of organisms, and evaluate the therapeutic effects and mechanisms of drugs (Zhang et al. 2020). The integration of network pharmacology and metabolomics provides new insights into disease mechanisms and the discovery of new drugs by using computational and experimental tools.

It is widely used for studying liver fibrogenesis progression in animals treated with carbon tetrachloride (CCl_4). Therefore, our study used a mouse model of liver fibrotic injury induced by CCl_4 to investigate the therapeutic effect of EGT on liver fibrosis and its mechanism based on metabonomics and network pharmacology. First, metabonomics was performed to analyze the metabolic biomarkers and key pathways. Secondly, the potential targets of EGT alleviating liver fibrosis and key signaling pathways were determined through network pharmacology. In addition, the common targets of metabonomics and network pharmacology were examined to investigate the potential mechanism of EGT against liver fibrosis. In this study, a theoretical foundation has been laid for accurate screening of metabolic biomarkers, as well as in-depth study of mechanisms and clinical application of EGT.

2 | Materials and Methods

2.1 | Reagents and Chemicals

EGT was purchased from Shanghai Yien Chemical Technology Co., Ltd. (Shanghai, China) and was dissolved in 0.9% NaCl (Yueren Biotechnology Co., Ltd., Dongguan, China). Olive oil and CCl_4 (≥99.0%) were obtained from Shanghai Macklin Biochemical Co., Ltd. (Shanghai, China). The kits for detecting aspartate aminotransferase (AST) and alanine aminotransferase (ALT) were obtained from Jiancheng Biological Engineering Institute (Nanjing, China). Total bilirubin (TBIL) was purchased

from Elabscience Biotechnology Co., Ltd. (Wuhan, China). ELISA kits of mouse Laminin (LN) and hydroxyproline (Hyp) were purchased from Nanjing Camillo Biological Engineering Co., Ltd. (Nanjing, China). Reverse transcription kit and Perfectstart Uni RT&qPCR kit were obtained from TransGen Biotech Co., Ltd. (Beijing, China). The primers were synthesized from General Biol (Anhui, China). RIPA lysis buffer and BCA assay kit were obtained from Epizyme Biomedical Technology Co., Ltd (Shanghai, China). Primary antibodies against α-SMA (1:4000), Col-I (1:2000), Col-III (1:700), TGF-β (1:2500), Smad2 (1:300), Smad3 (1:4000) and β-actin (1:5000) were obtained from Proteintech Group, lnc. (Wuhan, China). Enhanced chemiluminescence kit was obtained from Vazyme Biotech Co., Ltd (Nanjing, China).

2.2 | Animal Treatments

All experimental procedures involving animals were rigorously performed in adherence to the international ethical guidelines and NIH guidelines for the care and use of laboratory animals, which were granted approval by the Animal Ethics Committee of Shenyang Medical College. A total of 40 SPF male C57BL/6J mice, aged 6 to 7 weeks and weighing 17 to 22 g, were obtained from Beijing Weitonglihua Laboratory Animal Co., Ltd. (Certificate No. SCXK2021-0006, Beijing, China). Mice were raised in the Laboratory Animal Center of Shenyang Medical College under controlled conditions (12 h light/dark cycle at a temperature range of (24 ± 2)°C and a relative humidity of 60–70%. Mice had uninhibited access to both food and water.

After 7 days of adaptive feeding, 40 mice were randomly and equally divided into four groups. CCl_4 was dissolved in olive oil and EGT was dissolved in normal saline solution. The control group received an intraperitoneal (ip) administration of olive oil (2 mL/kg) twice a week, along with orally administration of normal saline solution (5 mL/kg/d). The CCl_4 model group was ip injected with 40% CCl_4 (2 mL/kg) twice a week and orally gavaged with normal saline solution (5 mL/kg/d). In addition to ip administration of CCl_4 twice a week, the low-dose EGT (CCl_4 + EGT-L) group was also gavaged with 5 mg/kg/d EGT, and the high-dose EGT group (CCl_4 + EGT-H) was gavaged with 10 mg/kg/d EGT. After 6 weeks of intervention, mice were anesthetized at 24 h after the last administration, the serum was obtained, and the liver was removed and weighed. A minor portion of the liver was fixed in 4% paraformaldehyde for histopathological analysis. The residual liver was stored at −80°C for detection.

2.3 | Biochemical Analysis of Liver Function

According to the manufacturer's instructions, serum levels of ALT, AST, and TBIL were detected using bio-diagnostic kits, and the absorbance at 510 nm was detected using a multifunctional microplate reader (Molecular Devices, Sunnyvale, California, USA). The serum levels of Hyp and LN were detected by ELISA kits. The absorbance at 450 nm was measured. The concentration of each index was calculated from the standard curve.

2.4 | Histological Examination

After fixation with 4% paraformaldehyde for 72 h, liver tissues were embedded in paraffin and cut into paraffin sections of 3–5 μm thickness, followed by deparaffinized in xylene and rehydrating in graded ethanol. After that, the sections underwent staining procedures with Hematoxylin and Eosin (H&E), Masson's trichrome (MT), and Sirius red (SR), respectively. The histopathological changes were observed under an optical microscope (Nikon, Tokyo, Japan).

2.5 | Immunohistochemical Staining

Paraffin sections were deparaffinized and rehydrated. Antigen repair process was performed by high-temperature heating repair method. After washing three times with PBS, 3% H_2O_2 solution was added and incubated for 25 min at room temperature in the dark. Following three washes with PBS, the sections were blocked with non-immune animal serum for 20 min before being incubated with primary antibodies against α-SMA, Col-I, and Col-III overnight at 4°C. We then washed the sections three times with PBS, and further incubated them with a secondary antibody for 1 h at room temperature. Following three additional washes with PBS, DAB Color Development Kit (Beyotime Biotechnology, Shanghai, China) was dripped on the sections. The color development was controlled under the microscope and terminated by rinsing with tap water. After 3 min of hematoxylin staining, the stained sections were dehydrated with gradient alcohol and xylene and sealed with neutral gum, then examined using optical microscope.

2.6 | qPCR Analysis

We extracted total RNA from liver tissue with Trizol reagent (Vazyme biotech Co., Ltd, Nanjing, China), and RNA concentration was quantified by a spectrophotometer (Thermo, Waltham, Massachusetts, USA). Reverse transcription of liver RNA was performed using the Reverse Transcription Kit. Gene expression was determined by qPCR with Perfectstart Uni RT&qPCR Kit using a 7500 fast real-time PCR system (ABI-7500, Carlsbad, California, USA), normalized against *Gapdh*. Primers for the qPCR were in Table S1.

2.7 | Western Blot Analysis

Using RIPA lysis buffer (containing 1% PMSF), liver tissue was lysed by RIPA lysis buffer with 1% PMSF (protease inhibitor) and then centrifuged at 12,000 g (20 min) at 4°C. BCA was used to determine the protein concentration. A total of 20 μg of protein was separated by 10% SDS-PAGE, transferred to PVDF membranes, blocked for 20 min with fast blocking buffer, and subsequently incubated overnight with primary antibodies at 4°C. TBST-washed membranes were further incubated with HRP-conjugated secondary antibodies (1:1000) for 1 h. Followed by enhanced chemiluminescence reagent for visualizing, the protein bands were imaged by automatic chemiluminescence imaging system (Tanon 5200, Shanghai, China). Image density was quantified by Image J software, and normalized against β-actin.

2.8 | Metabonomics Analysis

Frozen liver tissue was thawed gradually at 4°C, and prechilled mixture of methanol, acetonitrile, and water (2:2:1, v/v) was added. After mixing, the solution was sonicated for 30 min, incubated at −20°C for 10 min. After centrifuging at 14,000 g for 20 min at 4°C, the supernatant underwent evaporation until dryness, then was reconstituted with an aqueous solution of acetonitrile (acetonitrile: water = 1:1, v/v, 100 μL). After vortexing, the mixture was centrifuged at 14,000 g for 15 min at 4°C, and the supernatant 2 μL was injected for analysis.

In order to conduct the metabolomics testing, LC–MS/MS was used along with a Vanquish ultra-high-performance liquid chromatography (UHPLC, Thermo) coupled to a Q Exactive mass spectrometer (Thermo). Acquity UPLC BEH Amide column (1.7 μm, 2.1 mm × 100 mm, Waters, Manchester, UK) was used for chromatographic separation. The mobile phases A was deionized water with 25 mM ammonium acetate and 25 mM ammonia and mobile phases B was acetonitrile. A column temperature of 25°C was used with a flow rate of 0.3 mL/min. The linear elution gradient was optimized as follows: 0–1.5 min (98% B); 1.5–12 min (98–2% B); 12–14 min (2% B); 14–14.1 min (2–98% B); 14.1–17 min (98% B). During the analysis, samples were kept in the autosampler at 4°C.

Electrospray ionization (ESI) positive and negative ion modes were used for mass spectrometry analysis (Thermo). The ESI setting parameters included nebulizer gas and heater gas at 60 psi, curtain gas (CUR) at 30 psi, ion spray voltage floating at ±5500 V, and ion source temperature at 600°C. The scan range of the first mass-to-charge ratio was 80–1200 Da with a resolution of 60,000 and a scan accumulation time of 100 ms. The scan range of the second mass-to-charge ratio was 70–1200 Da with a resolution of 30,000 and a scan accumulation time of 50 ms.

Progenesis QI software (Waters) was used to preprocess the raw data for peak alignment, selection, deconvolution, and normalization. The quality of data was evaluated by total ion chromatogram (TIC) and Pearson correlation analysis of QC samples. Orthogonal partial least squares-discriminant analysis (OPLS-DA) was analyzed using SIMCA 17.0 software (Umetrics, Malmo, Sweden). Metabolites with Variable Importance for the Projection (VIP) > 1 was screened for significant difference. The differential metabolites were imported into "Wu Kong" platform (https://omicsolution.org/) for Mfuzz analysis. The identified metabolites were then analyzed for pathway enrichment using MetaboAnalyst (www.metaboanalyst.ca).

2.9 | Target Acquisition and Analysis

The targets of liver fibrosis were searched by inputting the keywords "hepatic fibrosis" into GeneCards Database (http://www.genecards.org/). The compound structure of EGT were downloaded from the Pubchem Server (https://pubchem.ncbi.nlm.nih.gov/). The chemical structure was then imported into Swiss Target Prediction (http://www.swisstargetprediction.ch/) to predict the targets. The common targets were obtained by Venny 2.1 online software (https://bioinfogp.cnb.csic.es/tools/venny/). Enrichment analyses of GO and Kyoto Encyclopedia of Genes and Genomes (KEGG) pathway were performed by Metascape software (http://metascape.org/) to obtain the potential mechanisms of EGT treating hepatic fibrosis, with $p < 0.05$ as the significance threshold. STRING 12.0 (https://string-db.org/) and Cytoscape 3.9.1 were used to establish the protein–protein interaction (PPI) network.

2.10 | Integrated Analysis of Metabolomics and Network Pharmacology

Using MetScape, a Cytoscape 3.9.1 plug-in, we obtained the compound-reaction-enzyme-gene network and identified the key metabolites. The genes obtained from the network diagram and the common genes of EGT against hepatic fibrosis were intersected to obtain the core targets.

2.11 | Molecular Docking

The 3D structure of EGT (PubChem CID: 5351619) was acquired from PubChem Compound (https://www.ncbi.nlm.nih.gov/pccompound). After energy-minimization, the compound was transformed into MOL2 format using Chem3D (CambridgeSoft, Cambridge, Massachusetts, USA). Then, the format of EGT was converted into pdbqt format using AutoDockTools 1.5.6 (The Scripps Research Institute, San Diego, California, USA). PDB database (https://www.rcsb.org/) provided the crystal structures of targets. These structures were processed with Pymol 2.3 software (DeLano Scientific LLC, Palo Alto, California, USA), then transformed into pdbqt format after removing water molecules, adding hydrogen atoms and charges, and setting atom types by AutoDockTools 1.5.6. The processed EGT was employed as a ligand, and the target was a receptor. The docking process was performed using AutoDock Vina (The Scripps Research Institute). The molecular docking results were analyzed, and the visualization of the compound-target interaction was performed using PyMol 2.3 software.

2.12 | Statistical Analysis

Statistical analysis was performed using SPSS 26.0 (IBM, Armonk, New York, USA) and GraphPad Prism 9.0 (GraphPad Software, San Diego, California, USA) software. Normality test and homogeneity of variance test were performed on the experimental data. Data were presented as mean ± SD. Differences between groups were compare using one-way ANOVA with LSD-*t* for pairwise comparisons. $p < 0.05$ was indicate a statistically significant difference.

3 | Results

3.1 | Effects of EGT on Liver Coefficient and Gross Morphology in CCl_4-Treated Mice

The chemical structure of EGT was shown in Figure 1A. As shown in Figure 1B, a notable rise in liver coefficient was observed in CCl_4 mice compared to the control group ($p < 0.01$). Nevertheless, treatment with EGT significantly decreased

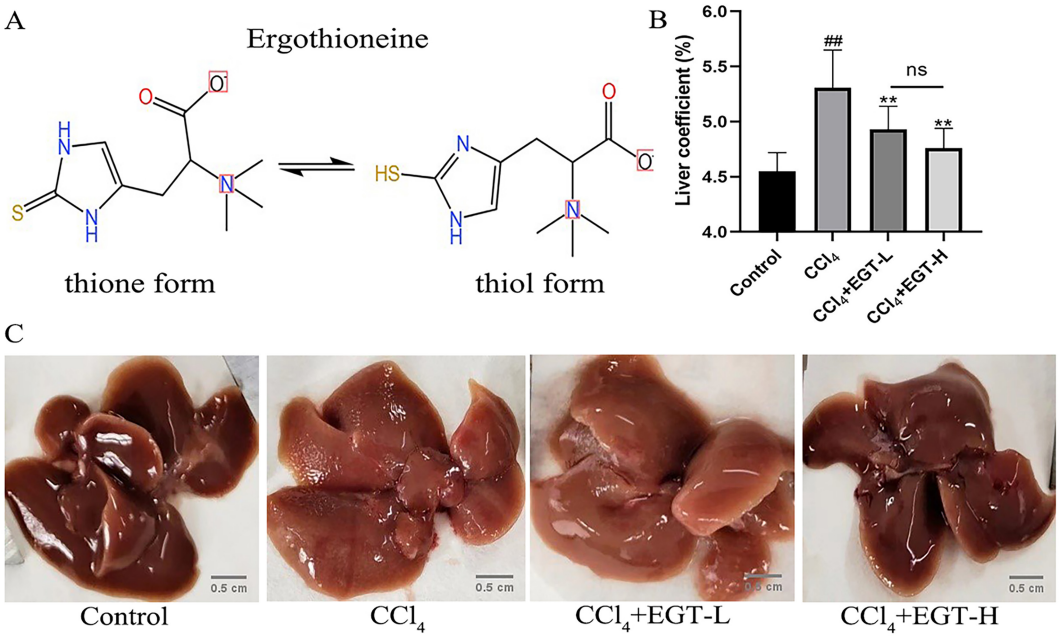

FIGURE 1 | Effect of EGT treatment on liver coefficient and gross morphology of liver in CCl_4 mice. (A) The chemical structure of EGT and its tautomer. (B) Effect of EGT on liver coefficient ($n = 10$). (C) Effect of EGT on gross morphology of liver. Data were expressed as means ± SD. $^{\#\#}p < 0.01$, compared with the control group; $^{*}p < 0.05$, $^{**}p < 0.01$, compared with the CCl_4 group, or compared between the two EGT groups.

the liver coefficient in CCl_4 mice ($p < 0.01$). Effects of EGT on gross morphology of liver were shown in Figure 1C. The liver in the control group had normal morphology and showed dark red, with smooth surface. Swollen liver was found in the CCl_4 group, which was enlarged in size, lighter in color, lusterless in appearance, and with granular nodules on the surface. After EGT treatment, there were fewer small granular nodules in the CCl_4+EGT-L group. And in the CCl_4+EGT-H group, the liver was dark red and the degree of fibrosis was significantly reduced. These results indicated that EGT mitigated hepatic damage and fibrosis induced by CCl_4 in mice.

3.2 | EGT Decreased Serum Levels of ALT, AST, and TBIL in CCl_4-Treated Mice

ALT, AST, and TBIL are commonly used biomarkers for liver damage. As shown in Figure 2A–C, serum levels of ALT, AST, and TBIL were significantly increased in the CCl_4 group compared to the control group ($p < 0.01$). However, these indicators were significantly decreased by EGT compared with CCl_4 ($p < 0.05$), and the levels of AST and TBIL were lower in the CCl_4+EGT-H group compared with the CCl_4+EGT-L group ($p < 0.05$). These findings indicated that EGT improved liver function by down-regulating AST, ALT, and TBIL levels.

3.3 | EGT Decreased Serum LN and HyP Levels in CCl_4-Treated Mice

LN and HyP are used to evaluate the degree of liver fibrosis. The serum levels of LN and Hyp in mice were detected by ELISA (Figure 2D,E). Results showed that the levels of LN and HyP were significantly higher in the CCl_4 group compared to the control group ($p < 0.01$). After treatment with 5 or 10 mg/kg EGT, serum LN and HyP levels were significantly lower compared with the CCl_4 group ($p < 0.01$). These results indicated that EGT could improve liver fibrosis.

3.4 | EGT Ameliorated CCl_4-Induced Hepatic Pathological Damage in Mice

H&E, SR, and MT staining were used to perform hepatic pathological examinations (Figure 3). Macroscopic examination showed that, in the control group, the structure of hepatic lobules was clear, hepatic cells were neatly arranged, only a small amount of collagen fibers was observed, and no fibrous tissue hyperplasia was observed in the hepatic lobules. However, pathological changes were observed in the CCl_4 group, the irregular hepatic lobules, swelling, degeneration, necrosis, and inflammatory cell infiltration of hepatic cells were observed. And a large amount of collagen fibers was deposited in liver tissues, the normal structure of lobules was destroyed, and pseudolobules were formed. EGT treatment substantially reduced the degeneration, necrosis, and disordered organization of hepatic cells induced by CCl_4, as well as fiber connective tissue, pseudolobules, and inflammatory infiltration. These results indicated that EGT exerted a hepatoprotective effect, which in the EGT-H (10 mg/kg) group was better than that in the EGT-L (5 mg/kg) group.

3.5 | EGT Decreased the Expressions of Pro-Fibrotic Genes α-SMA, Col-I, and Col-III in CCl_4-Treated Mice

To further investigate the role of EGT in liver fibrosis, the expressions of pro-fibrotic genes α-SMA, Col-I, and

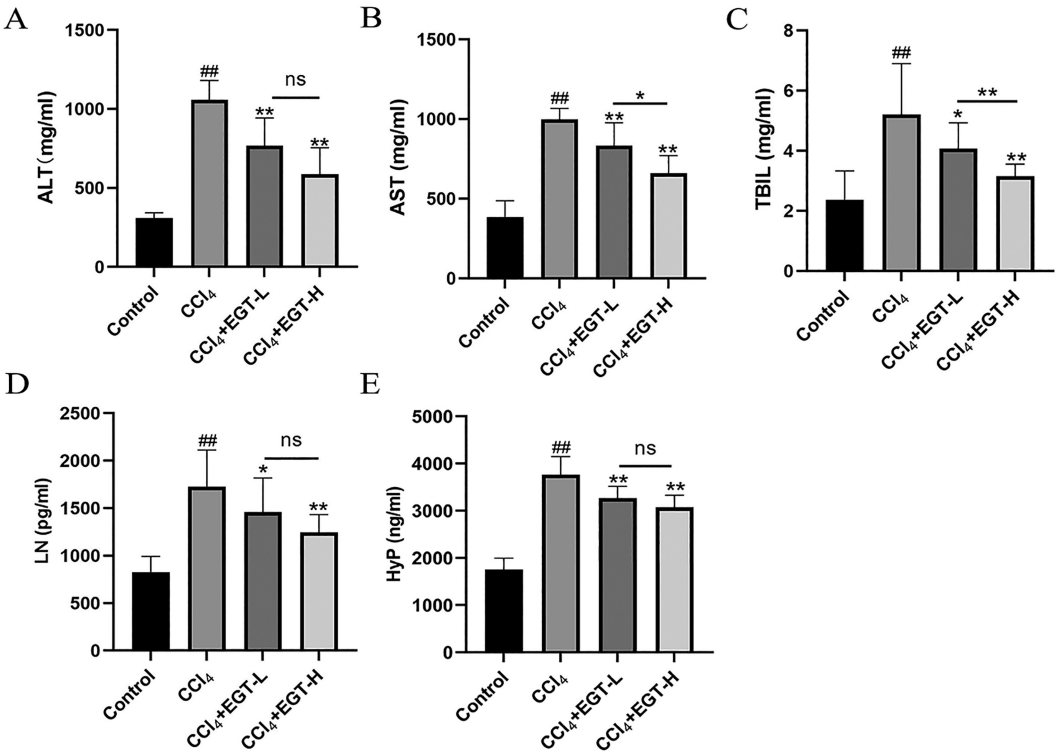

FIGURE 2 | Effect of EGT treatment on liver function and fibrosis indicators in CCl_4 mice. (A–C) Effect of EGT on liver function was assessed by serum levels of ALT, AST, and TBIL ($n = 6$). (D–E) Effect of EGT on liver fibrosis was assessed by serum levels of LN and HyP (n = 6). Data were expressed as means ± SD. $^{\#\#}p < 0.01$, compared with the control group; $^{*}p < 0.05$, $^{**}p < 0.01$, compared with the CCl_4 group, or compared between the two EGT groups.

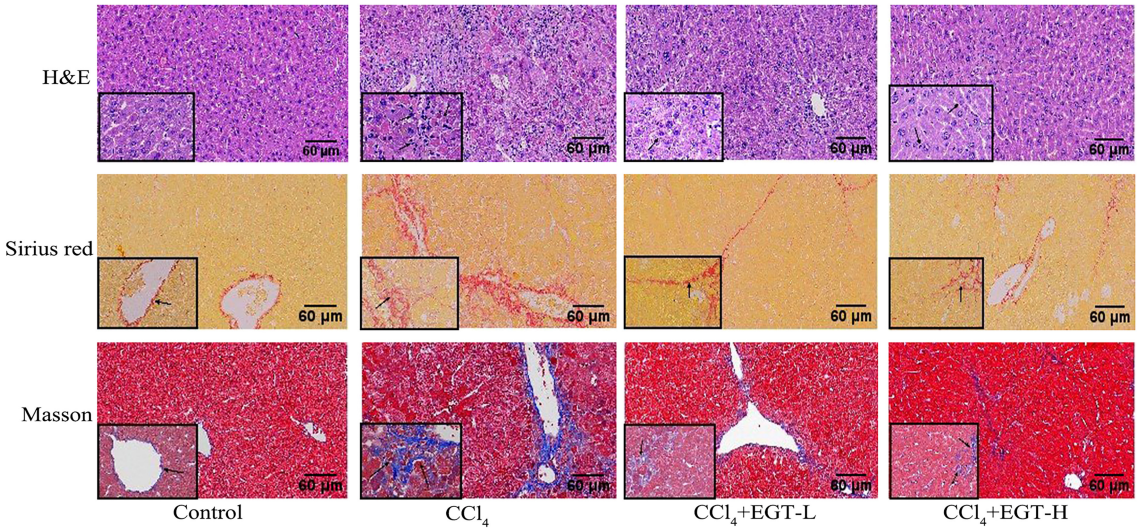

FIGURE 3 | Effect of EGT treatment on the liver pathological changes in CCl_4 mice. Liver sections were stained with H&E, Sirius Red and Masson. Representative photographs showed the liver pathological changes observed by macroscopic examination (original magnification, ×200).

Col-III in liver tissues were examined by immunohistochemical staining (Figure 4A). The positive expressions of α-SMA, Col-I, and Col-III were significantly increased in the CCl_4 group compared with the control group ($p < 0.05$). EGT treatment significantly attenuated increases in the levels of these indicators ($p < 0.05$). Consistently, the mRNA and protein expressions of *Acta2* (α-SMA), *Col1a1* (Col-I), and *Col3a1* (Col-III) were also decreased in CCl_4 mice treated with EGT, and the higher dose of EGT had a better hepatoprotective effect (Figure 4B,C).

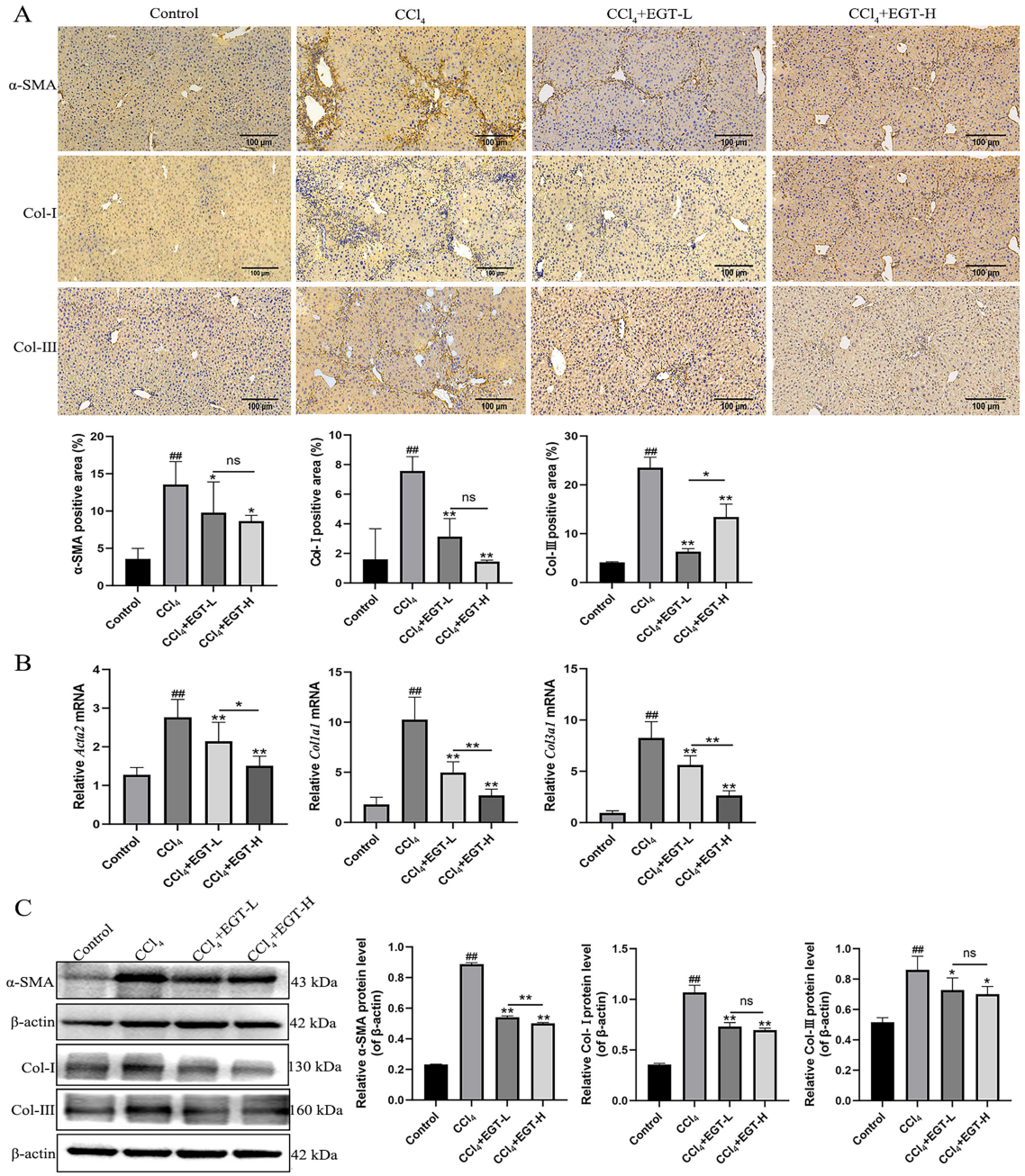

FIGURE 4 | Effect of EGT on the expression levels of α-SMA, Col-I and Col-III. (A) Immunohistochemistry staining (original magnification, ×100), (B) qPCR and (C) Western blot were used to detect the mRNA and protein expression levels of *Acta2* (α-SMA), *Col1a1* (Col-I) and *Col3a1* (Col-III). Data were expressed as means ± SD (n = 6). $^{\#\#}p < 0.01$, compared with the control group; $^{*}p < 0.05$, $^{**}p < 0.01$, compared with the CCl_4 group, or compared between the two EGT groups.

3.6 | EGT Decreased the Expressions of Pro-Inflammatory Cytokines IL-6, IL-1β, and TNF-α in CCl_4-Treated Mice

It was shown in Figure 5 that CCl_4 significantly increased the mRNA levels of *Il6*, *Il1b*, and *Tnf* in the liver compared with the control group ($p < 0.05$). EGT treatment significantly attenuated increases in the levels of *Il6*, *Il1b*, and *Tnf*, and the higher dose of EGT had a better hepatoprotective effect ($p < 0.05$), indicating that EGT could depress inflammatory response.

3.7 | EGT Down-Regulated the TGF-β Signaling Pathway in CCl_4-Treated Mice

TGF-β signaling pathway has been suggested to be key fibrogenic pathway that drives HSCs activation and induces ECM production (Dewidar et al. 2019; Yang et al. 2022). Therefore, we further explored whether EGT alleviated liver fibrosis through TGF-β signaling pathway. As shown in Figure 6A, compared with the control group, the mRNA and protein levels of *Tgfb1* (TGF-β) in the liver were significantly increased in

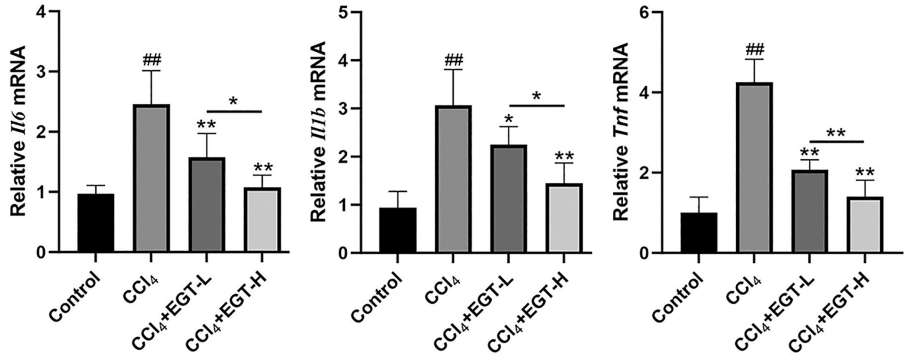

FIGURE 5 | Effect of EGT on liver inflammatory biomarkers IL-6, IL-1β, and TNF-α. The mRNA levels of *Il6*, *Il1b* and *Tnf* in the liver were detected by qPCR. Data are presented as means ± SD (n = 6). $^{\#\#}p < 0.01$, compared with the control group; $^{*}p < 0.05$, $^{**}p < 0.01$, compared with the CCl_4 group, or compared between the two EGT groups.

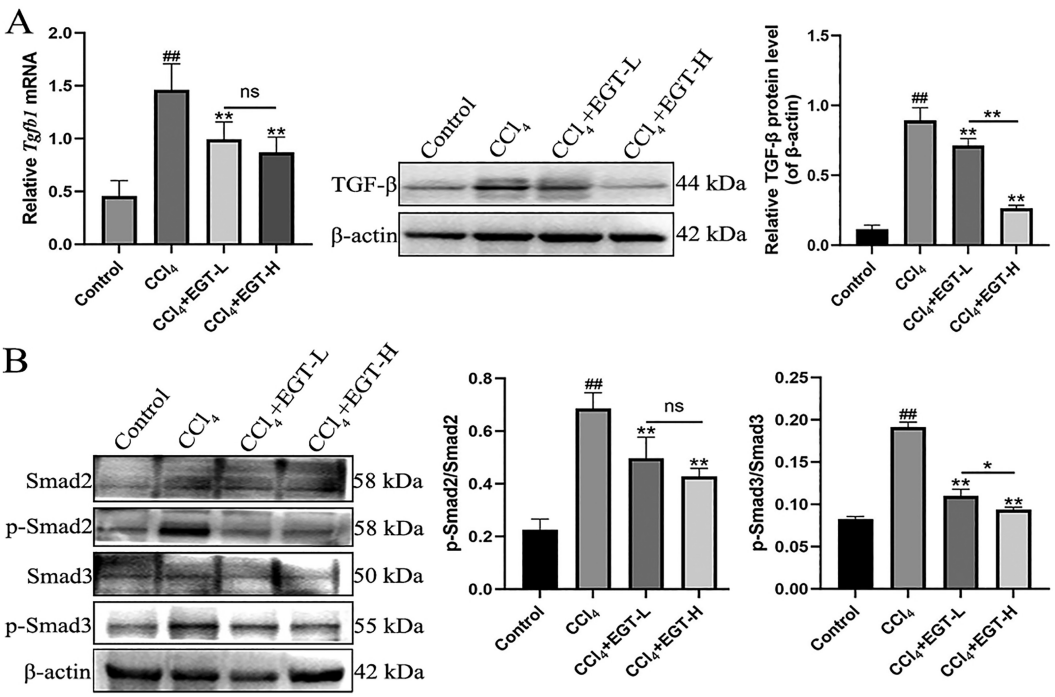

FIGURE 6 | Effect of EGT on TGF-β/Smads signaling pathway. (A) The mRNA and protein expression levels of *Tgfb1* (TGF-β) were detected by qPCR and Western blot. (B) The protein expression levels of Smad2, p-Smad2, Smad3, and p-Smad3 were detected by Western blot. Data were expressed as means ± SD (n = 6). $^{\#\#}p < 0.01$, compared with the control group; $^{*}p < 0.05$, $^{**}p < 0.01$, compared with the CCl_4 group, or compared between the two EGT groups.

the CCl_4 group ($p < 0.05$). EGT treatment significantly decreased the mRNA and protein levels of *Tgfb1* in CCl_4 mice and the higher dose of EGT had a better hepatoprotective effect ($p < 0.01$). TGF-β exerts its biological effects by activating downstream mediators Smad2 and Smad3. As shown in Figure 6B, compared with the control group, the protein levels of p-Smad2 and p-Smad3 were significantly increased in the CCl_4 group ($p < 0.05$). The protein levels of Smad2, p-Smad2, Smad3 and p-Smad3 in the CCl_4+EGT groups were significantly lower than those in the CCl_4 group, and the higher dose of EGT had a better hepatoprotective effect ($p < 0.05$). Taken together, these results indicates that EGT may alleviate liver fibrosis in mice by down-regulating the TGF-β/Smads signaling pathway.

3.8 | Effects of EGT on Metabolite Profiling in CCl_4-Treated Mice

To further analyze the potential pathological mechanism of EGT treatment of liver fibrosis, metabolomics analysis was performed in the control, CCl_4, and CCl_4+EGT-H groups, with five samples in each group. TICs of QC samples in the positive and negative ionization modes showed that the retention time and response strength of each chromatographic peak basically overlapped (Figure S1). Pearson correlation analysis between QC samples was performed, and the Pearson correlation coefficients were all >0.995 (Figure S2). These results indicated that the experiment had good stability and repeatability.

The metabolic variations were also determined using a multivariate OPLS-DA model (Figure 7). The three quantitative parameters included $R^2X = 0.788$, $R^2Y = 0.999$ and $Q^2 = 0.959$ of control vs. CCl_4, $R^2X = 0.932$, $R^2Y = 1.000$ and $Q^2 = 0.94$ of CCl_4 vs. CCl_4+EGT-H, and $R^2X = 0.627$, $R^2Y = 0.999$ and $Q^2 = 0.956$ of control vs. CCl_4+EGT-H, indicating good reliability and high predictability of the model. Furthermore, results of permutation test indicated good robustness of the original model had and no over-fitting.

A total of 819 metabolites were identified. VIP > 1 was used as the screening criteria for significant differential metabolites; and 495 differential metabolites were identified by pairwise comparison of control, CCl_4, and CCl_4+EGT-H groups. Exogenous metabolites identified using HMDB database were eliminated. Finally, 350 endogenous differential metabolites were obtained.

To further understand the dynamic changes of endogenous metabolites, Mfuzz analysis was conducted, and the endogenous differential metabolites were classified into nine patterns. As illustrated in Figure 8A, metabolites of Clusters 1 and 3 were down-regulated in the CCl_4 group, but up-regulated after EGT treatment. Metabolites of Clusters 5 and 9 were up-regulated in the CCl_4 group, but down-regulated after EGT treatment. A total of 41 differential metabolites in Clusters 1 and 3, and 38 differential metabolites in Clusters 5 and 9 were analyzed for pathway enrichment using MetaboAnalyst. KEGG analysis showed that purine metabolism, glycerophospholipid metabolism, pantothenate and CoA biosynthesis were significant in Clusters 1 and 3 (Raw $p < 0.5$, Impact>0.1) (Figure 8B), histidine metabolism, sphingolipid metabolism, and phenylalanine, tyrosine and tryptophan biosynthesis were significant in Clusters 5 and 9 (Raw $p < 0.5$, Impact>0.1) (Figure 8C), which may be identified as the core signaling pathways involved in the potential mechanism of EGT in the treatment of liver fibrosis (Table S2).

3.9 | Network Analysis of EGT Against Liver Fibrosis

A total of 100 targets of EGT were predicted based on Swiss Target Prediction. As shown in Figure 9A, among the categories

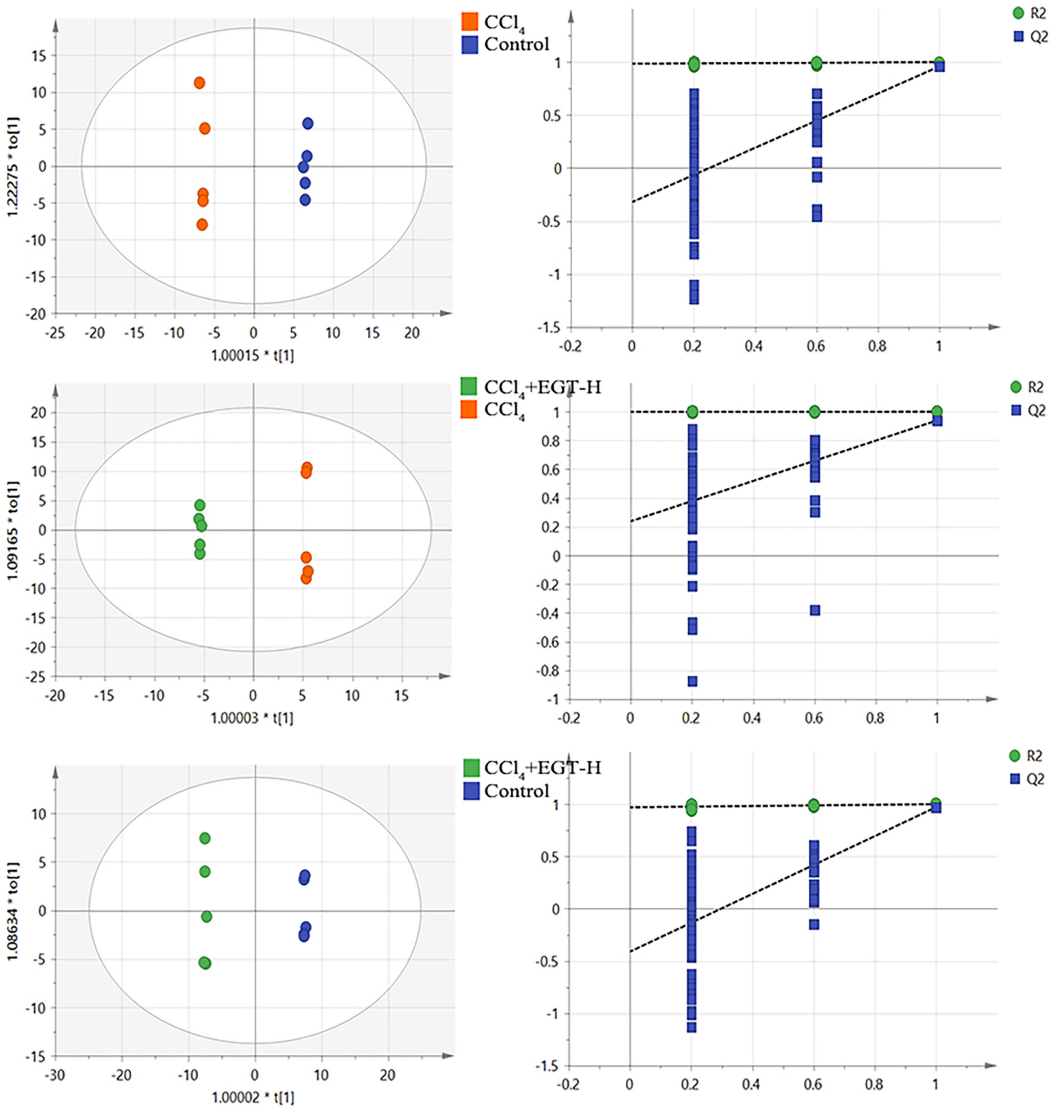

FIGURE 7 | OPLS-DA model and permutation test summary for pair-wise comparison.

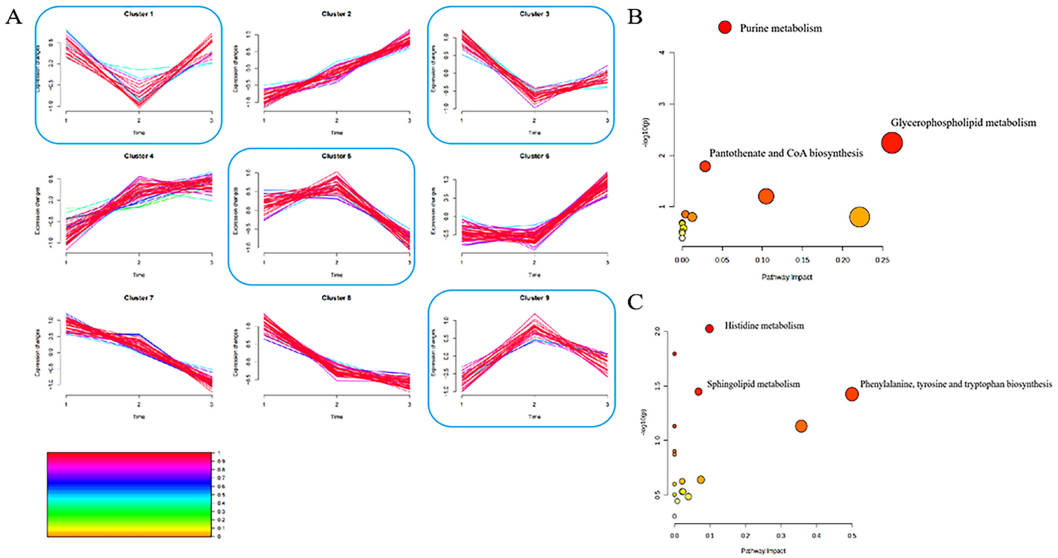

FIGURE 8 | Effect of EGT on the dynamic changes of endogenous differential metabolites. (A) Clustering analysis was performed using Mfuzz; (B) KEGG analysis of differential metabolites in Cluster 1 and 3; (C) KEGG analysis of differential metabolites in Cluster 5 and 9.

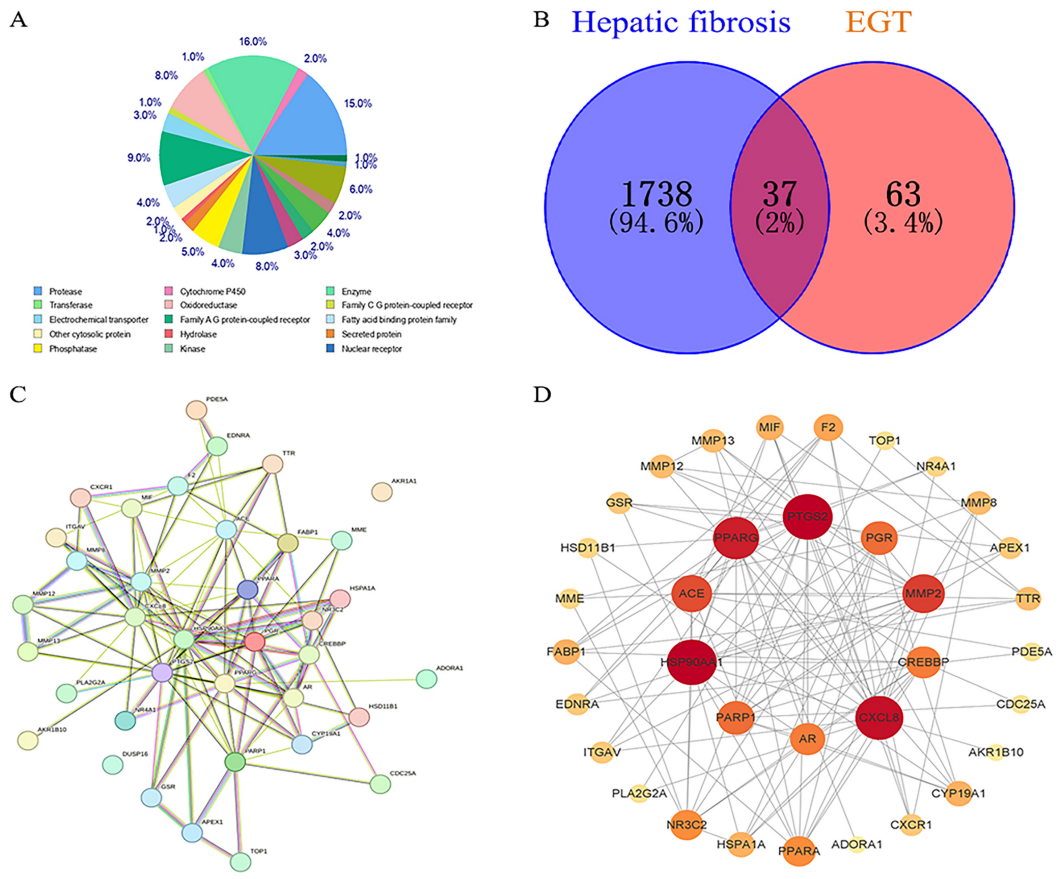

FIGURE 9 | Screening of targets of EGT against hepatic fibrosis. (A) The categories of predicted target genes of EGT; (B) Venn diagram for the predicted targets of EGT and hepatic fibrosis; (C) The PPI network of EGT treatment on hepatic fibrosis; (D) Visual analysis of PPI network by Cytoscape.

of target genes, transferase (16.0%), protease (15.0%), oxidoreductase (8.0%), and nuclear receptor (8.0%) accounted for a relatively high proportion. And 1775 targets of hepatic fibrosis were predicted based on GeneCards Database with Relevance score >5. The predicted targets were imported into Venny 2.1 software and 37 common targets were obtained (Figure 9B and Table S3).

A PPI network of common targets was established by STRING 12.0 (Figure 9C). The PPI network was then imported into Cytoscape for visual analysis (Figure 9D). The top 10 targets by the degree value were PTGS2, PGR, MMP2, CREBBP, CXCL8, AR, PARP1, HSP90AA1, ACE, and PPARG. These targets were central targets and acted as links connecting other targets.

Enrichment analysis of common targets was performed by Metascape software. $p < 0.05$ was set as the significance threshold. The top 20 terms of biological processes were shown in Figure 10A. The main biological processes included response to hormone, response to hypoxia, positive regulation of lipid metabolic process, collagen catabolic process, regulation of apoptotic process, inflammatory response, etc. In Figure 10B, six GO terms were enriched in cellular components, including ficolin-1-rich granule lumen, extracellular matrix, perinuclear region of cytoplasm, etc. In Figure 10C, 10 GO terms were enriched in molecular functions, including metalloendopeptidase activity, nuclear receptor activity, oxidoreductase activity, etc.

As shown in Figure 10D, nine pathways were obtained from KEGG enrichment analysis, including pathways in cancer, IL-17 signaling pathway, cAMP signaling pathway, alcoholic liver disease, NF-κB signaling pathway, etc.

3.10 | Integrated Analysis of Metabolomics and Network Pharmacology

To further explore the mechanism of EGT against liver fibrosis, 39 differential metabolites with KEGG IDs were analyzed by Metscape plug-in of Cytoscape 3.9.1 software, and compound-reaction-enzyme-gene networks were constructed (Figure 11A). The network comprised 550 nodes, including 87 metabolites (23 input metabolites), 95 reactions, 70 enzymes, and 275 genes. Based on Degree>4, Betweenness>5000, and Centroid valve >-30, nine key metabolites were screened, and eight of which were input metabolites, including xanthine, guanine, adenosine triphosphate (ATP), uridine, sphingosine, phosphatidylcholine (16:0/22:4 (7Z, 10Z, 13Z, 16Z)), 5-thymidylic acid, and phosphatidate (LysoPA (16:0/0:0)) (Table 1). As illustrated in Figure 11B, compared with the control group, xanthine, guanine, ATP, and uridine were significantly down-regulated in the CCl_4 group ($p < 0.05$), but were significantly up-regulated after EGT administration ($p < 0.05$). Sphingosine and phosphatidylcholine were significantly up-regulated in the CCl_4 group compared with the control group ($p < 0.05$), but were significantly down-regulated after EGT administration ($p < 0.05$).

A total of 275 targets were obtained from compound-reaction-enzyme-gene networks, which interacted with the 37 targets predicted in network pharmacology, and the common target PLA2G2A was screened.

A molecular docking study was conducted to investigate the possibility of interaction between EGT and PLA2G2A (Figure 11C). It was found that EGT exhibited hydrogen-bonding interactions with GLY29, GLY31, and ASP48. The binding energies of EGT towards PLA2G2A was −7.3 kcal/mol. The docking result indicated that EGT might act directly on PLA2G2A to ameliorate liver fibrosis.

4 | Discussion

Chronic liver diseases of different etiologies are a major global health burden, and the progression of chronic liver diseases involves persistent activation of inflammatory response and liver fibrogenesis (Parola and Pinzani 2019). The development of liver fibrosis correlates with impaired liver function, and determines quality of life and prognosis (Roehlen, Crouchet, and Baumert 2020). Recent evidence has convincingly demonstrated that fibrosis is reversible. Development of new drugs that can prevent and treat liver fibrosis is of great importance. EGT was used in this study to investigate the hepatoprotective effect against liver fibrosis in classical CCl_4-treated mice.

The diet-derived anti-oxidant EGT has therapeutic potential. In vivo studies have reported that EGT is related to a lower risk of cognition impairment (Kondoh et al. 2022), cardiometabolic disease, and mortality (Smith et al. 2020). Researchers have suggested that EGT is an adaptive anti-oxidant, does not interfere with the roles of ROS in healthy tissues, but exhibits anti-oxidant and cytoprotective properties only under conditions of oxidative stress (Halliwell, Tang, and Cheah 2023; Paul 2022). Therefore, in addition to being a safe, all-natural anti-oxidant derived from diet, its therapeutic potential looks promising, while research on its potential in mitigating liver fibrosis is lacking.

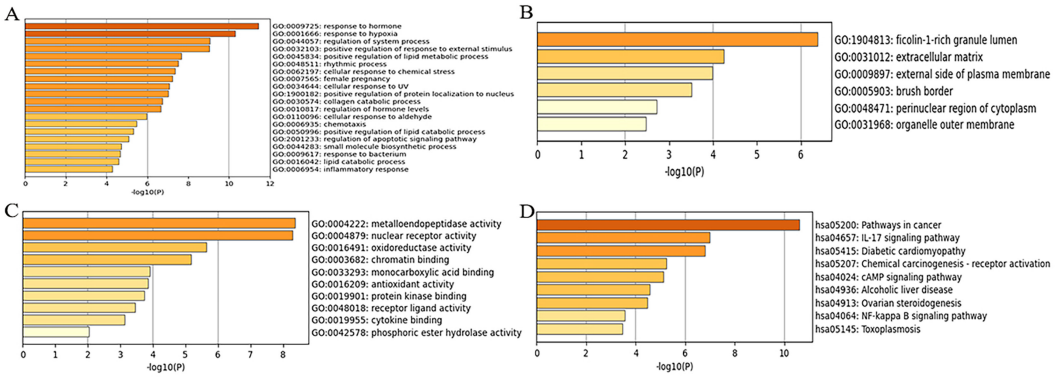

FIGURE 10 | Enrichment analysis of common targets of EGT against hepatic fibrosis. (A–C) The GO enrichment results of biological process (A), cellular component (B), and molecular function (C); (D) KEGG enrichment analysis.

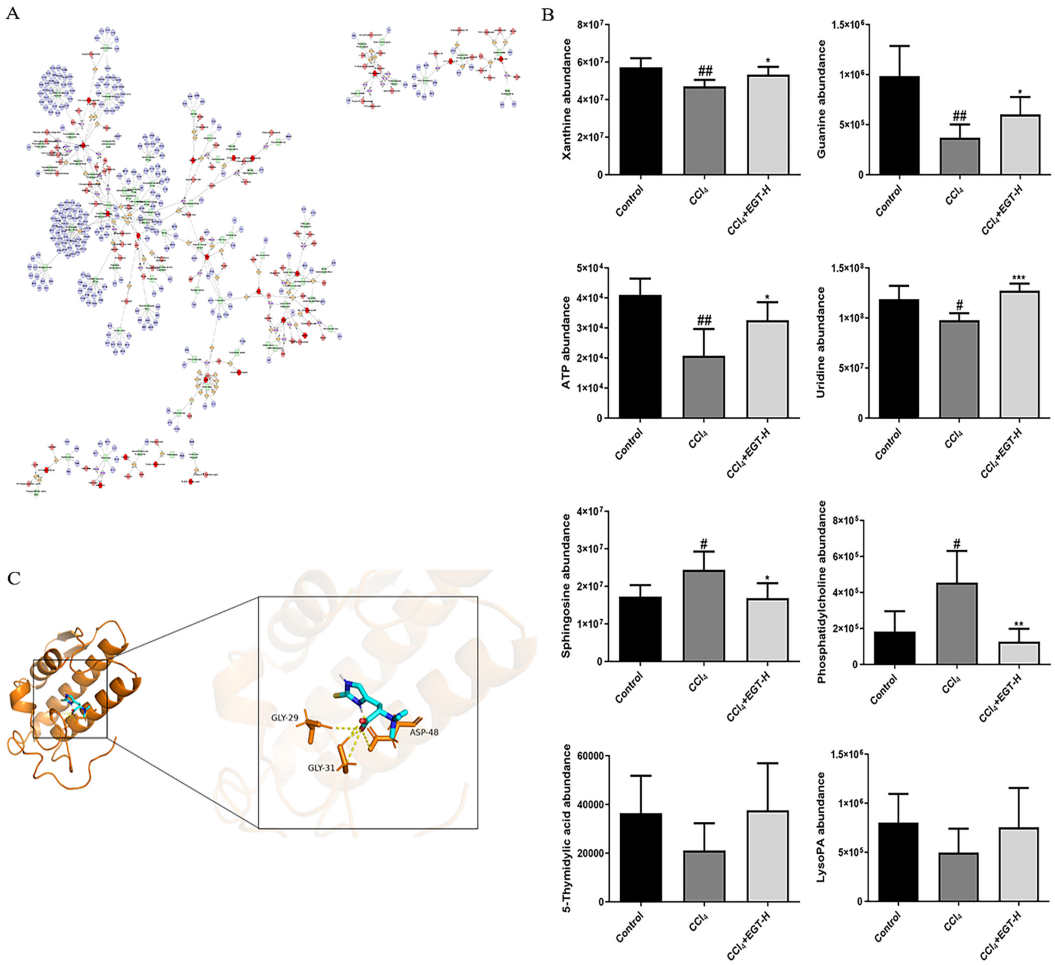

FIGURE 11 | Enrichment analysis of common targets of EGT against hepatic fibrosis. (A) EGT-regulated metabolite-reaction-enzyme-gene network; (B) The contents of key metabolites ($n = 5$); (C) Molecular docking of the interaction between EGT and PLA2G2A. $^{\#}p < 0.05$, $^{\#\#}p < 0.01$, compared with the control group; $^{*}p < 0.05$, $^{**}p < 0.01$, compared with the CCl_4 group.

TABLE 1 | Key differential metabolites in metabolite-reaction-enzyme-gene network.

Metabolites	KEGG IDs	Degree	Centroid valve	Betweenness
Xanthine	C00385	7	−5	6517
Guanine	C00242	5	−9	11,315
ATP	C00002	7	−9	64,066
Uridine	C00299	12	−12	18,036
Sphingosine	C00319	5	−4	13,863
Phosphatidylcholine (16:0/22:4 (7Z, 10Z, 13Z, 16Z))	C00157	11	−28	43,952
5-thymidylic acid	C00364	6	−8	101,481
LysoPA (16:0/0:0)	C00416	10	−28	52,533

In the present study, liver function parameters (ALT, AST, and TBIL) and liver fibrosis markers (LN and HyP) were detected, and elevated serum activities of these markers along with liver pathological damage were observed in CCl_4 mice. EGT treatment significantly attenuated these effects, which indicates that EGT has evident effect on protecting liver function and relieving fibrosis. In hepatic fibrogenesis, ECM components are excessively accumulated, and activated HSCs are identified as being the main sources of ECM (Kisseleva and Brenner 2021). The α-SMA was served as an indicator of activated HSCs (Tsuchida and Friedman 2017). Col-I and Col-III are fundamental components of ECM (Kisseleva and Brenner 2021). Here, EGT treatment also

significantly decreased the expressions of α-SMA, Col-I, and Col-III in CCl_4 mice, thereby inhibiting ECM deposition and ameliorating liver fibrosis. Nevertheless, the exact mechanism by which EGT improves liver fibrosis remains unclear.

It is thought that inflammation protects liver structure and function in response to a variety of factors, including ECM components and damage-associated molecular patterns, however, when harmful factors continue to be present, it can result in liver fibrosis (Caligiuri et al. 2021; Peiseler et al. 2022). A growing body of evidence suggests that EGT plays a protective role by alleviating inflammatory response (Cheah and Halliwell 2020; Liu et al. 2023). IL-6, IL-1β, and TNF-α are the key pro-inflammatory cytokines that drive liver fibrosis, and can facilitate the initiation process of HSC activation (Higashi, Friedman, and Hoshida 2017). In this study, we found that EGT treatment significantly attenuated increases in the mRNA levels of *Il6*, *Il1b* and *Tnf* in CCl_4 mice. This result is consistent with other reports (Dare, Channa, and Nadar 2021; Salama and Omar 2021). Dare, Channa, and Nadar (2021) reported that after induction of diabetes, EGT alleviated hepatic oxidative damage by activating Sirt1/Nrf2 signaling pathway, and reduced hepatic inflammation by down-regulating NF-κB and TNF-α expression. Salama and Omar (2021) also demonstrated that NF-κB-p65 nuclear translocation as well as TNF-α and IL-6 levels were significantly reduced by EGT, indicating its mitigating effects of EGT on the hepatocellular inflammatory response. Studies of other inflammatory diseases have also reported that EGT can reduce the IL-1β level (Koh et al. 2021; Wang et al. 2023). These findings provide support for the anti-inflammatory effect of EGT in mitigating liver fibrosis, and its anti-inflammatory mechanism deserves further investigation.

During acute and chronic liver injury, TGF-β is activated from deposits in the ECM and expressed and released from various cell types such as endothelial cells, macrophages, hepatocytes and platelets (Ghafoory et al. 2018; Schon and Weiskirchen 2014). TGF-β proteins exist in three isoforms, TGF-β1, 2, and 3, and TGF-β1 is the most widely investigated isoform in liver fibrogenesis (Xu et al. 2016). TGF-β1 promotes fibrogenesis by inducing myofibroblast formation, and also inhibits ECM degradation by inhibiting matrix metalloproteinases (MMP) and promoting protease inhibitors (Xu et al. 2016). TGF-β exerts its biological effects by activating downstream mediators Smad2 and Smad3. The phosphorylated Smad2 and Smad3 form heterocomplexes with Smad4, which thereafter translocate into the nucleus to regulate the transcription of multiple target genes, such as fibrogenic genes (Col-I and Col-III) and markers (α-SMA and E-cadherin) (Carthy 2018). Therefore, TGF-β/Smads signaling pathway is an important therapeutic target for liver fibrosis treatment. Mu et al. (2018) reported that exogenous TGF-β1 treatment significantly increased the expressions of Col-I, α-SMA, p-Smad2 and p-Smad3 in human hepatic stellate cell line. Overexpression of TGF-β promotes Col-I deposition by decreasing MMP1 level and increasing COL1A1 level (Shen et al. 2022). However, pharmacological blocking of TGF-β ameliorates liver fibrosis in rats (de Gouville et al. 2005). Dare, Channa, and Nadar (2021) also reported that EGT alleviated hepatic fibrosis by downregulating TGF-β1 expression. This result is consistent with our data. Here, our study showed that EGT treatment significantly decreased the expressions of TGF-β, Smad2, p-Smad2, Smad3 and p-Smad3 in CCl_4 mice and the higher dose of EGT had a better hepatoprotective effect. And the decreased expression of α-SMA, Col-I and Col-III induced by EGT may be due to the inhibition of TGF-β/Smads signaling pathway. Taken together, these results significantly indicating that inhibition of TGF-β/Smads signaling may be a key mechanism by which EGT exerted its antifibrotic effects on CCl_4-treated mice.

Metabolomics analysis was carried out to investigate the potential pathological mechanism of EGT treatment of liver fibrosis. KEGG pathway analysis demonstrated that purine metabolism, glycerophospholipid metabolism, pantothenate and CoA biosynthesis, histidine metabolism, sphingolipid metabolism, and phenylalanine, tyrosine and tryptophan biosynthesis were core signaling pathways, which may be potential mechanisms of EGT against liver fibrosis. Importantly, purine metabolism is the most significant differential metabolic pathway in this study. This result is consistent with the latest research that the concentration of purine metabolites was negatively correlated with liver damage indicators in a high-fat diet (HFD) mouse model (Qiu et al. 2023). The key metabolites Xanthine, Guanine, and ATP screened by MetScape analysis in the present study are intermediate products of purine metabolism. The decreased levels of these metabolites in the CCl_4 group indicate impaired *de novo* purine synthesis and elevated purine catabolism, which leads to the accumulation of excess uric acid. Uric acid is the end metabolite derived from purine metabolism, which is associated with the severity of liver damage. A cross-sectional study indicated a positive correlation between uric acid levels and liver steatosis and fibrosis (Duan et al. 2022). Hyperuricemia model of mice showed that uric acid induction significantly increased Col-I mRNA expression and the number of HSCs, therefore, augmenting liver fibrosis (Sari et al. 2020). However, EGT alleviates liver fibrosis by increasing the levels of metabolites Xanthine, Guanine, and ATP. Collectively, purine metabolism and related pathways may be potential targets of EGT against liver fibrosis, which deserve further study.

Glycerophospholipid metabolism is the second significantly differential metabolic pathway. The key metabolite phosphatidylcholine is involved in glycerophospholipid metabolism. The increased level of phosphatidylcholine in the CCl_4 group is inhibited by EGT treatment, indicating that EGT mitigates liver fibrosis by suppressing glycerophospholipid metabolism. The findings align with previous studies. Lin et al. (2022) also found that the mechanism of tormentic acid alleviating liver fibrosis is related to the inhibition of glycerophospholipid metabolism pathway by regulating the synthesis of phosphatidylcholine. Didymin isolated from *Origanum vulgare* L. can ameliorate liver fibrosis by inhibiting the glycerophospholipid metabolism with decreased synthesis of phosphatidylcholines and phosphatidylethanolamines (Li et al. 2022). It has been confirmed that glycerophospholipids are the key phospholipids in eukaryotic membranes, which are essential for maintaining the structural integrity and functionality of these membranes (Gibellini and Smith 2010). CCl_4 exposure can strongly induce oxidative damage and inflammatory response, resulting in excessive glycerophospholipids in hepatocytes, ultimately destroying cell membrane structure. However, EGT treatment significantly reverses these changes and alleviates liver fibrosis.

Sphingolipid metabolism is another significantly differential metabolic pathway. The key metabolite sphingosine is an important signaling lipid in sphingolipid metabolism. The increased level of sphingosine in the CCl_4 group is inhibited by EGT treatment, indicating that EGT alleviates liver fibrosis by inhibiting the sphingolipid metabolism. As key sphingolipids, sphingosine and ceramide, along with their metabolic enzymes, exert major intracellular effects to significantly alter immune responses, which may change the pathogenesis and natural history of liver fibrosis (Ishay et al. 2020). Sphingosine kinase (SphK) can convert sphingosine into sphingosine-1-phosphate (S1P), a potent signaling substance (Park et al. 2020). Accumulating evidence has shown that in fibrotic liver tissue, increased hepatic SphK expression induces the elevation of hepatic S1P level, which is an accomplice in liver pathobiology, including NALFD, acute liver failure, and liver fibrosis (Kawai et al. 2022; King et al. 2017). Therefore, sphingolipid pathway may be an emerging new potential target for EGT against liver fibrosis.

Pantothenate and CoA biosynthesis is down-regulated after CCl_4 treatment. This result is consistent with a study about evaluating CoA metabolism in mouse models of NASH, and the results demonstrate that hepatic CoA metabolism is impaired in NASH mice, resulting in decreased free CoA content, activation of caspase-2, and increased liver cell apoptosis (Machado et al. 2016). Therefore, EGT may alleviate liver fibrosis by increasing free CoA content.

Network analysis of the potential mechanism of EGT in the treatment of liver fibrosis showed that IL-17, cAMP and NF-κB signaling pathways may be important molecular mechanisms. IL-17A signal is involved in the development of liver fibrosis by activating HSCs and increasing the release of proinflammatory cytokines, indicating that IL-17A may be a promising strategy for treating fibrosis (Zhang et al. 2015). cAMP, a key second messenger molecule, is involved in inflammation, metabolism, and development of fibrosis. As a protective molecular pathway, cAMP signaling is inhibited during liver injury (Wahlang et al. 2018). NF-κB plays a critical role in inflammation. In diethylnitrosamine-induced liver fibrosis rat model, NF-κBp65 nuclear translocation was significantly promoted with a decrease in the cytoplasmic fraction (Rodríguez et al. 2021). Ba et al. (2021) suggested that N-Myc downstream-regulated gene 2 (NDRG2) might modulate TGF-β1 expression through the NF-κB pathway, offering a new therapeutic target for liver fibrosis. Collectively, EGT may play an anti-inflammatory role through IL-17, cAMP and NF-κB signaling pathways, thereby alleviating liver fibrosis.

An analysis combining metabolomics, network pharmacology, and molecular docking indicates that PLA2G2A may be a potential target for EGT to alleviate hepatic fibrosis. PLA2 (Phospholipase A_2) has been reported to hydrolyze low-density lipoproteins (LDL), which promotes the production of pro-inflammatory lipids such as lysophospholipids and eicosanoids, thereby promotes collagen accumulation and fibrosis development (Oestvang and Johansen 2006). PLA2G2A (Phospholipase A_2 group IIA), a member of secretory phospholipases highly expressed in the liver, plays important roles in inflammation, atherogenesis, metabolic response, and cancer (Kuefner et al. 2021). PLA2G2A is one of the important enzymes in glycerophospholipid metabolism, which catalyzes the hydrolysis of phospholipids and releases free fatty acids and lysophospholipids (Kuefner et al. 2021). Lin et al. (2022) reported that tormentic acid alleviated liver fibrosis by inhibiting glycerophospholipid metabolism pathway through down-regulating the expression of PLA2G2A. Loki zupa formula was reported to exert anti-inflammatory effects by blocking IL-6/PLA2G2A signalling (Mohammadtursun et al. 2020). Jaiswal et al. (2023) reported that PLA2G2A was increased in the idiopathic pulmonary fibrosis fibroblasts, and the high expressed PLA2G2A fibroblasts could upregulate the inflammatory and fibrosis-related pathways, such as TGF-β signaling pathway and ECM-receptor interaction. Levick et al. (2006) reported that daily treatment of spontaneously hypertensive rats with a PLA2G2A inhibitor (KH064) prevented the increases of perivascular and interstitial collagen in the left ventricle of rat hearts. Iyer et al. (2012) reported that diet-induced obesity caused overexpression and secretion of PLA2G2A from immune cells in adipose tissue and oral administration of KH064 prevented its overexpression and the increased macrophage infiltration. These results indicate that PLA2G2A may have an important role in inflammation and fibrosis, and that its inhibitors may be useful in alleviating liver fibrosis. In our study, we found that EGT mitigates liver fibrosis by suppressing glycerophospholipid metabolism through inhibiting the synthesis of phosphatidylcholine. Collectively, these data suggest that EGT may regulate the glycerophosphatidic metabolism pathway through inhibiting PLA2G2A, which inhibits the TGF-β/Smads pathway to play an anti-inflammatory role, thereby alleviating liver fibrosis. However, the molecular mechanism necessitates further investigation.

In summary, this study reveals that EGT can alleviate liver fibrosis by inhibiting the expression of α-SMA, Col-I, and Col-III to reduce ECM deposition, and its antifibrotic mechanism is related to reducing inflammatory response and inhibiting TGF-β/Smads signaling pathway. Moreover, an integrated analysis of metabolomics and network pharmacology was performed to investigate the therapeutic mechanism of EGT alleviating liver fibrosis. Metabolomics results indicate that purine metabolism, glycerophospholipid metabolism, pantothenate and CoA biosynthesis, histidine metabolism, sphingolipid metabolism, and phenylalanine, tyrosine and tryptophan biosynthesis were core signaling pathways, and eight key metabolites, including xanthine, guanine, ATP, Uridine, sphingosine, 5-thymidylic acid, phosphatidylcholine and LysoPA (16:0/0:0), were screened. Network pharmacology analysis demonstrates that IL-17, cAMP and NF-κB signaling pathways may be the potential key mechanisms by which EGT alleviates liver fibrosis through anti-inflammatory effects. Integrated analysis reveals that PLA2G2A may be a promising target for EGT. EGT may inhibit the glycerophospholipid metabolism through PLA2G2A to inhibit the TGF-β/Smads signaling pathway, thereby alleviating fibrosis. Taken together, the present study provides novel prospectives on the pharmacological mechanism of EGT in liver fibrosis and lays a theoretical basis for the in-depth investigations of mechanisms and clinical application of EGT.

Ethics Statement

This study was approved by the Animal Ethics Committee of Shenyang Medical College.

Conflicts of Interest

The authors declare no conflicts of interest.

Data Availability Statement

The data that support the findings of this study are available on request from the corresponding author. The data are not publicly available due to privacy or ethical restrictions.

References

Ames, B. N. 2018. "Prolonging Healthy Aging: Longevity Vitamins and Proteins." *Proceedings of the National Academy of Sciences of the United States of America* 115, no. 43: 10836–10844. https://doi.org/10.1073/pnas.1809045115.

Asrani, S. K., H. Devarbhavi, J. Eaton, and P. S. Kamath. 2019. "Burden of Liver Diseases in the World." *Journal of Hepatology* 70, no. 1: 151–171. https://doi.org/10.1016/j.jhep.2018.09.014.

Aydın, M. M., and K. C. Akçalı. 2018. "Liver fibrosis." *Turkish Journal of Gastroenterology* 29, no. 1: 14–21. https://doi.org/10.5152/tjg.2018.17330.

Ba, H. Z., Z. H. Liang, H. S. Kim, and W. Cao. 2021. "*TGF-β1* can Be Regulated by *NDRG2* via the NF-κB Pathway in Hypoxia-Induced Liver Fibrosis." *Annals of Translational Medicine* 9, no. 6: 505. https://doi.org/10.21037/atm-21-1298.

Banerjee, P., N. Gaddam, V. Chandler, and S. Chakraborty. 2023. "Oxidative Stress-Induced Liver Damage and Remodeling of the Liver Vasculature." *American Journal of Pathology* 193, no. 10: 1400–1414. https://doi.org/10.1016/j.ajpath.2023.06.002.

Borodina, I., L. C. Kenny, C. M. McCarthy, et al. 2020. "The Biology of Ergothioneine, an Antioxidant Nutraceutical." *Nutrition Research Reviews* 33, no. 2: 190–217. https://doi.org/10.1017/S0954422419000301.

Caligiuri, A., A. Gentilini, M. Pastore, S. Gitto, and F. Marra. 2021. "Cellular and Molecular Mechanisms Underlying Liver Fibrosis Regression." *Cells* 10, no. 10: 2759. https://doi.org/10.3390/cells10102759.

Campana, L., and J. P. Iredale. 2017. "Regression of Liver Fibrosis." *Seminars in Liver Disease* 37, no. 1: 1–10. https://doi.org/10.1055/s-0036-1597816.

Carthy, J. M. 2018. "TGFβ Signaling and the Control of Myofibroblast Differentiation: Implications for Chronic Inflammatory Disorders." *Journal of Cellular Physiology* 233, no. 1: 98–106. https://doi.org/10.1002/jcp.25879.

Charan, H. V., D. K. Dwivedi, S. Khan, and G. Jena. 2022. "Mechanisms of NLRP3 Inflammasome-Mediated Hepatic Stellate Cell Activation: Therapeutic Potential for Liver Fibrosis." *Genes & Diseases* 10, no. 2: 480–494. https://doi.org/10.1016/j.gendis.2021.12.006.

Cheah, I. K., and B. Halliwell. 2020. "Could Ergothioneine aid in the Treatment of Coronavirus Patients?." *Antioxidants (Basel, Switzerland)* 9, no. 7: 595. https://doi.org/10.3390/antiox9070595.

Cheah, I. K., R. Tang, P. Ye, T. S. Yew, K. H. Lim, and B. Halliwell. 2016. "Liver Ergothioneine Accumulation in a Guinea pig Model of non-alcoholic Fatty Liver Disease. A Possible Mechanism of Defence?." *Free Radical Research* 50, no. 1: 14–25. https://doi.org/10.3109/10715762.2015.1099642.

Cheah, I. K., R. M. Tang, T. S. Yew, K. H. Lim, and B. Halliwell. 2017. "Administration of Pure Ergothioneine to Healthy Human Subjects: Uptake, Metabolism, and Effects on Biomarkers of Oxidative Damage and Inflammation." *Antioxidants & Redox Signaling* 26, no. 5: 193–206. https://doi.org/10.1089/ars.2016.6778.

Chen, Q., R. Zhou, C. Yang, et al. 2023. "Ergothioneine Attenuates Varicocele-Induced Testicular Damage by Upregulating HSP90AA1 in Rats." *Journal of Biochemical and Molecular Toxicology* 37, no. 4: e23301. https://doi.org/10.1002/jbt.23301.

Cheng, Q., C. Li, C. F. Yang, et al. 2019. "Methyl Ferulic Acid Attenuates Liver Fibrosis and Hepatic Stellate Cell Activation Through the TGF-β1/Smad and NOX4/ROS Pathways." *Chemico-Biological Interactions* 299: 131–139. https://doi.org/10.1016/j.cbi.2018.12.006.

Dare, A., M. L. Channa, and A. Nadar. 2021. "L-Ergothioneine and Metformin Alleviates Liver Injury in Experimental Type-2 Diabetic Rats via Reduction of Oxidative Stress, Inflammation, and Hypertriglyceridemia." *Canadian Journal of Physiology and Pharmacology* 99, no. 11: 1137–1147. https://doi.org/10.1139/cjpp-2021-0247.

de Gouville, A. C., V. Boullay, G. Krysa, et al. 2005. "Inhibition of TGF-Beta Signaling by an ALK5 Inhibitor Protects Rats From Dimethylnitrosamine-Induced Liver Fibrosis." *British Journal of Pharmacology* 145, no. 2: 166–177. https://doi.org/10.1038/sj.bjp.0706172.

de Gregorio, E., A. Colell, A. Morales, and M. Marí. 2020. "Relevance of SIRT1-NF-κB Axis as Therapeutic Target to Ameliorate Inflammation in Liver Disease." *International Journal of Molecular Sciences* 21, no. 11: 3858. https://doi.org/10.3390/ijms21113858.

Deiana, M., A. Rosa, V. Casu, R. Piga, M. Assunta Dessì, and O. I. Aruoma. 2004. "L-Ergothioneine Modulates Oxidative Damage in the Kidney and Liver of Rats in Vivo: Studies Upon the Profile of Polyunsaturated Fatty Acids." *Clinical Nutrition* 23, no. 2: 183–193. https://doi.org/10.1016/S0261-5614(03)00108-0.

Dewidar, B., C. Meyer, S. Dooley, and A. N. Meindl-Beinker. 2019. "TGF-β in Hepatic Stellate Cell Activation and Liver Fibrogenesis-Updated 2019." *Cells* 8, no. 11: 1419. https://doi.org/10.3390/cells8111419.

Duan, H., R. Zhang, X. Chen, et al. 2022. "Associations of Uric Acid With Liver Steatosis and Fibrosis Applying Vibration Controlled Transient Elastography in the United States: A Nationwide Cross-Section Study." *Frontiers in Endocrinology* 13: 930224. https://doi.org/10.3389/fendo.2022.930224.

Fu, T. T., and L. Shen. 2022. "Ergothioneine as a Natural Antioxidant Against Oxidative Stress-Related Diseases." *Frontiers in Pharmacology* 13: 850813. https://doi.org/10.3389/fphar.2022.850813.

Ghafoory, S., R. Varshney, T. Robison, et al. 2018. "Platelet TGF-β1 Deficiency Decreases Liver Fibrosis in a Mouse Model of Liver Injury." *Blood Advances* 2, no. 5: 470–480. https://doi.org/10.1182/bloodadvances.2017010868.

Gibellini, F., and T. K. Smith. 2010. "The Kennedy Pathway—De Novo Synthesis of Phosphatidylethanolamine and Phosphatidylcholine." *IUBMB Life* 62, no. 6: 414–428. https://doi.org/10.1002/iub.337.

Gründemann, D., L. Hartmann, and S. Flögel. 2022. "The Ergothioneine Transporter (ETT): Substrates and Locations, an Inventory." *FEBS Letters* 596, no. 10: 1252–1269. https://doi.org/10.1002/1873-3468.14269.

Halliwell, B., I. K. Cheah, and R. M. Y. Tang. 2018. "Ergothioneine - A Diet-Derived Antioxidant With Therapeutic Potential." *FEBS Letters* 592, no. 20: 3357–3366. https://doi.org/10.1002/1873-3468.13123.

Halliwell, B., R. M. Y. Tang, and I. K. Cheah. 2023. "Diet-Derived Antioxidants: The Special Case of Ergothioneine." *Annual Review of Food Science and Technology* 14: 323–345. https://doi.org/10.1146/annurev-food-060822-122236.

Higashi, T., S. L. Friedman, and Y. Hoshida. 2017. "Hepatic Stellate Cells as key Target in Liver Fibrosis." *Advanced Drug Delivery Reviews* 121: 27–42. https://doi.org/10.1016/j.addr.2017.05.007.

Ishay, Y., D. Nachman, T. Khoury, and Y. Ilan. 2020. "The Role of the Sphingolipid Pathway in Liver Fibrosis: An Emerging new Potential Target for Novel Therapies." *American Journal of Physiology-Cell Physiology* 318, no. 6: C1055–C1064. https://doi.org/10.1152/ajpcell.00003.2020.

Iyer, A., J. Lim, H. Poudyal, et al. 2012. "An Inhibitor of Phospholipase A2 Group IIA Modulates Adipocyte Signaling and Protects Against Diet-Induced Metabolic Syndrome in Rats." *Diabetes* 61, no. 9: 2320–2329. https://doi.org/10.2337/db11-1179.

Jaiswal, A., R. Rehman, J. Dutta, et al. 2023. "Cellular Distribution of Secreted Phospholipase A2 in Lungs of IPF Patients and Its Inhibition in Bleomycin-Induced Pulmonary Fibrosis in Mice." *Cells* 12, no. 7: 1044. https://doi.org/10.3390/cells12071044.

Kawai, H., Y. Osawa, M. Matsuda, et al. 2022. "Sphingosine-1-Phosphate Promotes Tumor Development and Liver Fibrosis in Mouse Model of Congestive Hepatopathy." *Hepatology* 76, no. 1: 112–125. https://doi.org/10.1002/hep.32256.

King, A., D. D. Houlihan, D. Kavanagh, et al. 2017. "Sphingosine-1-Phosphate Prevents Egress of Hematopoietic Stem Cells From Liver to Reduce Fibrosis." *Gastroenterology* 153, no. 1: 233–248.e16. https://doi.org/10.1053/j.gastro.2017.03.022.

Kisseleva, T., and D. Brenner. 2021. "Molecular and Cellular Mechanisms of Liver Fibrosis and Its Regression." *Nature Reviews. Gastroenterology & Hepatology* 18, no. 3: 151–166. https://doi.org/10.1038/s41575-020-00372-7.

Koh, S. S., S. C. Ooi, N. M. Lui, et al. 2021. "Effect of Ergothioneine on 7-Ketocholesterol-Induced Endothelial Injury." *Neuromolecular Medicine* 23, no. 1: 184–198. https://doi.org/10.1007/s12017-020-08620-4.

Kondoh, H., T. Teruya, M. Kameda, and M. Yanagida. 2022. "Decline of Ergothioneine in Frailty and Cognition Impairment." *FEBS Letters* 596, no. 10: 1270–1278. https://doi.org/10.1002/1873-3468.14299.

Kuefner, M. S., E. Stephenson, M. Savikj, et al. 2021. "Group IIA Secreted Phospholipase A2 (PLA2G2A) Augments Adipose Tissue Thermogenesis." *FASEB Journal* 35, no. 10: e21881. https://doi.org/10.1096/fj.202002481RR.

Levick, S., D. Loch, B. Rolfe, et al. 2006. "Antifibrotic Activity of an Inhibitor of Group IIA Secretory Phospholipase A2 in Young Spontaneously Hypertensive Rats." *Journal of Immunology* 176, no. 11: 7000–7007. https://doi.org/10.4049/jimmunol.176.11.7000.

Li, Y., C. Li, Y. Xiong, B. Fang, X. Lin, and Q. Huang. 2022. "Didymin Ameliorates Liver Fibrosis by Alleviating Endoplasmic Reticulum Stress and Glycerophospholipid Metabolism: Based on Transcriptomics and Metabolomics." *Drug Design, Development and Therapy* 16: 1713–1729. https://doi.org/10.2147/DDDT.S351092.

Lin, X., Y. Wei, Y. Li, et al. 2022. "Tormentic Acid Ameliorates Hepatic Fibrosis *in Vivo* by Inhibiting Glycerophospholipids Metabolism and PI3K/Akt/mTOR and NF-κB Pathways: Based on Transcriptomics and Metabolomics." *Frontiers in Pharmacology* 13: 801982. https://doi.org/10.3389/fphar.2022.801982.

Liu, Y., C. Wang, R. Liu, et al. 2023. "Adhesive Ergothioneine Hyaluronate gel Protects Against Radiation Gastroenteritis by Alleviating Apoptosis, Inflammation, and gut Microbiota Dysbiosis." *ACS Applied Materials & Interfaces* 15, no. 16: 19833–19846. https://doi.org/10.1021/acsami.2c23142.

Machado, M. V., L. Kruger, M. L. Jewell, et al. 2016. "Vitamin B5 and N-Acetylcysteine in Nonalcoholic Steatohepatitis: A Preclinical Study in a Dietary Mouse Model." *Digestive Diseases and Sciences* 61, no. 1: 137–148. https://doi.org/10.1007/s10620-015-3871-x.

Milito, A., M. Brancaccio, G. D'Argenio, and I. Castellano. 2019. "Natural Sulfur-Containing Compounds: An Alternative Therapeutic Strategy Against Liver Fibrosis." *Cells* 8, no. 11: 1356. https://doi.org/10.3390/cells8111356.

Mohammadtursun, N., Q. Li, M. Abuduwaki, et al. 2020. "Loki Zupa Alleviates Inflammatory and Fibrotic Responses in Cigarette Smoke Induced rat Model of Chronic Obstructive Pulmonary Disease." *Chinese Medicine* 15: 92. https://doi.org/10.1186/s13020-020-00373-3.

Mu, M., S. Zuo, R. M. Wu, et al. 2018. "Ferulic Acid Attenuates Liver Fibrosis and Hepatic Stellate Cell Activation via Inhibition of TGF-β/Smad Signaling Pathway." *Drug Design, Development and Therapy* 12: 4107–4115. https://doi.org/10.2147/DDDT.S186726.

Nishikawa, K., Y. Osawa, and K. Kimura. 2018. "Wnt/β-Catenin Signaling as a Potential Target for the Treatment of Liver Cirrhosis Using Antifibrotic Drugs." *International Journal of Molecular Sciences* 19, no. 10: 3103. https://doi.org/10.3390/ijms19103103.

Oestvang, J., and B. Johansen. 2006. "PhospholipaseA2: A key Regulator of Inflammatory Signalling and a Connector to Fibrosis Development in Atherosclerosis." *Biochimica et Biophysica Acta* 1761, no. 11: 1309–1316. https://doi.org/10.1016/j.bbalip.2006.06.003.

Park, W. J., J. H. Song, G. T. Kim, and T. S. Park. 2020. "Ceramide and Sphingosine 1-Phosphate in Liver Diseases." *Molecules and Cells* 43, no. 5: 419–430. https://doi.org/10.14348/molcells.2020.0054.

Parola, M., and M. Pinzani. 2019. "Liver Fibrosis: Pathophysiology, Pathogenetic Targets and Clinical Issues." *Molecular Aspects of Medicine* 65: 37–55. https://doi.org/10.1016/j.mam.2018.09.002.

Paul, B. D. 2022. "Ergothioneine: A Stress Vitamin With Sntiaging, Vascular, and Neuroprotective Roles?." *Antioxidants & Redox Signaling* 36, no. 16–18: 1306–1317. https://doi.org/10.1089/ars.2021.0043.

Peiseler, M., R. Schwabe, J. Hampe, P. Kubes, M. Heikenwälder, and F. Tacke. 2022. "Immune Mechanisms Linking Metabolic Injury to Inflammation and Fibrosis in Fatty Liver Disease - Novel Insights Into Cellular Communication Circuits." *Journal of Hepatology* 77, no. 4: 1136–1160. https://doi.org/10.1016/j.jhep.2022.06.012.

Qin, J., Z. Luo, Q. Wang, et al. 2023. "Integrating Metabonomics and Metagenomics Sequencing to Study the Anti-Liver Fibrosis Effects of Palmatine in *Corydalis Saxicola* Bunting." *Journal of Ethnopharmacology* 315: 116666. https://doi.org/10.1016/j.jep.2023.116666.

Qiu, J., L. Chen, L. Zhang, et al. 2023. "Xie Zhuo Tiao Zhi Formula Modulates Intestinal Microbiota and Liver Purine Metabolism to Suppress Hepatic Steatosis and Pyroptosis in NAFLD Therapy." *Phytomedicine: International Journal of Phytotherapy and Phytopharmacology* 121: 155111. https://doi.org/10.1016/j.phymed.2023.155111.

Rodríguez, M. J., M. Sabaj, G. Tolosa, et al. 2021. "Maresin-1 Prevents Liver Fibrosis by Targeting Nrf2 and NF-κB, Reducing Oxidative Stress and Inflammation." *Cells* 10, no. 12: 3406. https://doi.org/10.3390/cells10123406.

Roehlen, N., E. Crouchet, and T. F. Baumert. 2020. "Liver Fibrosis: Mechanistic Concepts and Therapeutic Perspectives." *Cells* 9, no. 4: 875. https://doi.org/10.3390/cells9040875.

Salama, S. A., and H. A. Omar. 2021. "Modulating NF-κB, MAPK, and PI3K/AKT Signaling by Ergothioneine Attenuates Iron Overload-Induced Hepatocellular Injury in Rats." *Journal of Biochemical and Molecular Toxicology* 35, no. 5: e22729. https://doi.org/10.1002/jbt.22729.

Sari, D. C. R., A. S. Soetoko, A. S. Soetoko, et al. 2020. "Uric Acid Induces Liver Fibrosis Through Activation of Inflammatory Mediators and Proliferating Hepatic Stellate Cell in Mice." *Medical Journal of Malaysia* 75, no. Suppl 1: 14–18.

Schon, H. T., and R. Weiskirchen. 2014. "Immunomodulatory Effects of Transforming Growth Factor-β in the Liver." *Hepatobiliary Surgery and Nutrition* 3, no. 6: 386–406. https://doi.org/10.3978/j.issn.2304-3881.2014.11.06.

Shen, J., Z. Wang, W. Zhao, et al. 2022. "TGF-β1 Induces Type I Collagen Deposition in Granulosa Cells via the AKT/GSK-3β Signaling Pathway-Mediated MMP1 Down-Regulation." *Reproductive Biology* 22, no. 4: 100705. https://doi.org/10.1016/j.repbio.2022.100705.

Smith, E., F. Ottosson, S. Hellstrand, et al. 2020. "Ergothioneine Is Associated With Reduced Mortality and Decreased Risk of Cardiovascular Disease." *Heart* 106, no. 9: 691–697. https://doi.org/10.1136/heartjnl-2019-315485.

Sun, M., and T. Kisseleva. 2015. "Reversibility of Liver Fibrosis." *Clinics and Research in Hepatology and Gastroenterology* 39, no. Suppl 1: S60–S63. https://doi.org/10.1016/j.clinre.2015.06.015.

Tang, R. M. Y., I. K. Cheah, T. S. K. Yew, and B. Halliwell. 2018. "Distribution and Accumulation of Dietary Ergothioneine and Its Metabolites in Mouse Tissues." *Scientific Reports* 8, no. 1: 1601. https://doi.org/10.1038/s41598-018-20021-z.

Tian, X., J. L. Thorne, and J. B. Moore. 2023. "Ergothioneine: An Underrecognised Dietary Micronutrient Required for Healthy Ageing?." *British Journal of Nutrition* 129, no. 1: 104–114. https://doi.org/10.1017/S0007114522003592.

Tsuchida, T., and S. L. Friedman. 2017. "Mechanisms of Hepatic Stellate Cell Activation." *Nature Reviews. Gastroenterology & Hepatology* 14, no. 7: 397–411. https://doi.org/10.1038/nrgastro.2017.38.

Wahlang, B., C. McClain, S. Barve, and L. Gobejishvili. 2018. "Role of cAMP and Phosphodiesterase Signaling in Liver Health and Disease." *Cellular Signalling* 49: 105–115. https://doi.org/10.1016/j.cellsig.2018.06.005.

Wang, Z., J. Ma, Z. Miao, et al. 2023. "Ergothioneine Inhibits the Progression of Osteoarthritis via the Sirt6/NF-κB Axis Both in Vitro and in Vivo." *International Immunopharmacology* 119: 110211. https://doi.org/10.1016/j.intimp.2023.110211.

Xu, F., C. Liu, D. Zhou, and L. Zhang. 2016. "TGF-β/SMAD Pathway and Its Regulation in Hepatic Fibrosis." *Journal of Jistochemistry and Cytochemistry* 64, no. 3: 157–167. https://doi.org/10.1369/0022155415627681.

Yang, Z., H. Zhang, M. Yin, et al. 2022. "TGF-β1/Smad3 Upregulates UCA1 to Promote Liver Fibrosis Through DKK1 and miR18a." *Journal of Molecular Medicine* 100, no. 10: 1465–1478. https://doi.org/10.1007/s00109-022-02248-6.

Zhang, W., Y. Chen, H. Jiang, et al. 2020. "Integrated Strategy for Accurately Screening Biomarkers Based on Metabolomics Coupled With Network Pharmacology." *Talanta* 211: 120710. https://doi.org/10.1016/j.talanta.2020.120710.

Zhang, Y., D. Huang, W. Gao, et al. 2015. "Lack of IL-17 Signaling Decreases Liver Fibrosis in Murine *Schistosomiasis Japonica*." *International Immunology* 27, no. 7: 317–325. https://doi.org/10.1093/intimm/dxv017.

Supporting Information

Additional supporting information can be found online in the Supporting Information section.